

Myocardial Edema as Detected by Pre-Contrast T1 and T2 CMR Delineates Area at Risk Associated With Acute Myocardial Infarction

Martin Ugander, MD, PhD,* Paul S. Bagi, BS,* Abiola J. Oki, BS,* Billy Chen, MD, PhD,* Li-Yueh Hsu, DSc,* Anthony H. Aletras, PhD,* Saurabh Shah, MS,† Andreas Greiser, PhD,‡ Peter Kellman, PhD,* Andrew E. Arai, MD*
Bethesda, Maryland; Chicago, Illinois; and Erlangen, Germany

OBJECTIVES The aim of this study was to determine whether cardiac magnetic resonance (CMR) in vivo T1 mapping can measure myocardial area at risk (AAR) compared with microspheres or T2 mapping CMR.

BACKGROUND If T2-weighted CMR is abnormal in the AAR due to edema related to myocardial ischemia, then T1-weighted CMR should also be able to detect and accurately quantify AAR.

METHODS Dogs (n = 9) underwent a 2-h coronary occlusion followed by 4 h of reperfusion. CMR of the left ventricle was performed for mapping of T1 and T2 prior to any contrast administration. AAR was defined as regions that had a T1 or T2 value (ms) >2 SD from remote myocardium, and regions with microsphere blood flow (ml/min/g) during occlusion <2 SD from remote myocardium. Infarct size was determined by triphenyltetrazolium chloride staining.

RESULTS The relaxation parameters T1 and T2 were increased in the AAR compared with remote myocardium (mean ± SD: T1, 1,133 ± 55 ms vs. 915 ± 33 ms; T2, 71 ± 6 ms vs. 49 ± 3 ms). On a slice-by-slice basis (n = 78 slices), AAR by T1 and T2 mapping correlated ($R^2 = 0.95$, $p < 0.001$) with good agreement (mean ± 2 SD: 0.4 ± 16.6% of slice). On a whole-heart analysis, T1 measurements of left ventricular mass, AAR, and myocardial salvage correlated to microsphere measures ($R^2 = 0.94$) with good agreement (mean ± 2 SD: -1.4 ± 11.2 g of myocardium). Corresponding T2 measurements of left ventricular mass, AAR, and salvage correlated to microsphere analysis ($R^2 = 0.96$; mean ± 2 SD: agreement 1.6 ± 9.2 g of myocardium). This yielded a median infarct size of 30% of the AAR (range 12% to 52% of AAR).

CONCLUSIONS For determining AAR after acute myocardial infarction, noncontrast T1 mapping and T2 mapping sequences yield similar quantitative results, and both agree well with microspheres. The relaxation properties T1 and T2 both change in a way that is consistent with the presence of myocardial edema following myocardial ischemia/reperfusion. (J Am Coll Cardiol Img 2012;5:596–603) © 2012 by the American College of Cardiology Foundation

From the *Cardiovascular and Pulmonary Branch, National Heart, Lung, and Blood Institute, National Institutes of Health, Department of Health and Human Services, Bethesda, Maryland; †Siemens Medical Solutions, Chicago, Illinois; and ‡Siemens AG Healthcare Sector, Erlangen, Germany. This work was funded by the Intramural Research Program of the National Heart, Lung, and Blood Institute, National Institutes of Health (1 Z01 HL004607-08 CE). Dr. Arai is a principal investigator on a U.S. government Cooperative Research and Development Agreement (CRADA) with Siemens Medical Solutions (HL-CR-05-004). All other authors have reported that they have no relationships relevant to the contents of this paper to disclose.

Manuscript received September 10, 2011; revised manuscript received December 16, 2011, accepted January 6, 2012.

Myocardial area at risk (AAR) is defined as myocardium that becomes ischemic upon coronary occlusion (1). Accurate quantification of AAR is important in studies aimed at determining the efficacy of infarct size reduction therapies. Measurement of AAR and infarct size allows determination of myocardial salvage—a measure of therapeutic efficacy (1).

Edema is a consequence of even short periods of myocardial ischemia (2). Myocardial T2 relaxation properties determined by cardiac magnetic resonance (CMR) are sensitive to changes in tissue water content (3). In vivo CMR can accurately delineate the AAR using a number of imaging

See page 604

techniques that utilize T2-weighting (4–9). Furthermore, ischemic injury also leads to an increase in myocardial T1, which is also related to increased tissue water content (3,10,11). Similarly, noncontrast T1-weighted CMR has been shown to be capable of quantifying the AAR ex vivo (12) and detecting regions of acute myocardial infarction in vivo (13). Notably, the in vivo study (13) did not try to differentiate between infarction and AAR. Recently, clinically relevant methods have been developed that can produce quantitative maps of both T1 (14) and T2 (15) with high signal to noise. The resulting images and parametric maps translate signal intensities into absolute T1 or T2 relaxation times, respectively. These methods have the potential to improve objectivity of T1 and T2 imaging.

The aim of this study was to determine the accuracy for quantifying AAR with clinically available T1 and T2 mapping sequences when compared with microsphere blood flow analysis as an independent reference standard. We hypothesized that if T2-weighted CMR is abnormal in the AAR due to edema related to myocardial ischemia, then T1-weighted CMR should also be able to detect and accurately quantify AAR.

METHODS

Animal preparation. Nine dogs weighing 10 to 15 kg were studied with institutional approval. Anesthesia was induced by subcutaneous acepromazine (0.2 mg/kg), followed by intravenous thiopental sodium (15 mg/kg). Anesthesia was sustained by inhaled isoflurane (0.5% to 2.0%). The animals were intubated and surgical preparation included venous catheters, arterial lines, a left atrial catheter, and a

snare around the left anterior descending coronary artery, typically positioned distal to the first diagonal branch. Coronary occlusion was maintained for 2 h. Fluorescent microspheres (IMT Stason, Irvine, California) were injected into the left atrium during simultaneous withdrawal of a reference femoral artery blood sample. Reperfusion was maintained for 4 h prior to commencing imaging. Animals were euthanized with potassium chloride following heparin administration.

CMR imaging. The entire left ventricle (LV) was imaged in contiguous short-axis slices at 1.5-T (Magnetom Avanto, Siemens Healthcare Sector, Erlangen, Germany) with an 8-channel coil prior to administration of any CMR contrast agents. Quantitative T1 mapping was performed with a Modified Look-Locker Inversion-Recovery (MOLLI) sequence (14) using the following typical imaging parameters: repetition time/echo time 220/1.14 ms; flip angle 35°; field of view 270 × 185 mm²; matrix 192 × 132 pixels; slice thickness 6 mm; parallel imaging factor 2; acquisition in late diastole on every other heartbeat; minimal inversion time 120 ms; increment 80 ms; voxel size 1.5 × 1.4 × 6.0 mm; temporal resolution 221 ms. The T1 mapping scheme included 3 acquisitions after the first inversion pulse, followed by a 3-heartbeat pause, a second inversion followed by 3 acquisitions, a second 3-heartbeat pause, and a third inversion for the last 5 acquisitions.

Quantitative T2 mapping was performed using a T2-prepared steady-state free precession (SSFP) sequence (15) and the following imaging parameters: repetition time/echo time 240/1.19 ms; flip angle 70°; field of view 270 × 185 mm²; matrix 192 × 132 pixels; slice thickness 6 mm; parallel imaging factor 2; acquisition in late diastole on every fourth heartbeat; T2 preparations: 0 ms, 24 ms, 55 ms, 90 ms, size 1.9 × 1.4 × 6.0 mm, temporal resolution 239 ms.

Image analysis. T1 pixel maps were generated using MRmap version 1.0 (SourceForge.net, Geeknet Inc., Fairfax County, Virginia) (16). T2 pixel maps were automatically generated on the MR scanner. T1 map and T2 map images were analyzed using the software Segment (version 1.8 R1289, Medviso, Lund, Sweden) (17). The epicardial and endocardial borders of the LV were manually delineated. AAR was semiautomatically identified as LV myocardium with pixel values (T1 or T2) >2 SD from remote myocardium. Spurious noncontiguous pixels comprising <10% of the LV myocardium were

ABBREVIATIONS AND ACRONYMS

AAR	= area at risk
ANOVA	= analysis of variance
CMR	= cardiac magnetic resonance
LV	= left ventricle/ventricular
SSFP	= steady-state free precession
TTC	= triphenyltetrazolium chloride

automatically excluded (18). Tissue weight in grams for imaging results was calculated as the volume of myocardium multiplied by the density of myocardium (1.05 g/cm^3). One observer performed all image analyses twice for assessment of intraobserver variability, and an additional blinded observer performed image analyses for assessment of interobserver variability. Overall image quality was excellent or good in all animals.

Histopathology preparation and quantification. After explantation, hearts were set in 2% agarose gel and sliced in the short-axis plane using a commercially available meat slicer. Slices were stained with 1% triphenyltetrazolium chloride (TTC) and then photographed. In the TTC-stained slices, the borders of the epicardium, endocardium, and nonstained regions were delineated manually to determine infarct size (19).

Microsphere analysis. Each slice was photographed, sectioned into 16 transmural radial sectors, and sent for quantification of blood flow (IMT Stason). T1 and T2 maps and microspheres were visually matched by comparing photographs of ex vivo slices with each in vivo image. This matching was performed blinded to the results of microsphere analysis. Microsphere blood flow analysis was performed blinded to the results of T1 and T2 data. Myocardial sectors with blood flow 2 SD below blood flow in remote myocardium was defined as AAR. Basal and apical slices were not used to determine the remote myocardial blood flow due to greater heterogeneity of flow measurements. The summed weight of sectors with blood flow below the 2-SD threshold was divided by the weight of all sectors in the slice to quantify the percent of slice comprising AAR. Salvaged myocardium was determined as AAR minus

infarct size by TTC. The use of the 2-SD threshold for both T1 and T2 maps and microspheres was postulated a priori, and was further determined to be reasonable upon visual inspection of the quality of the images and the microsphere data.

Statistical analysis. Statistical analysis was performed using SPSS version 17 (IBM, Somers, New York). Linear regression analysis was performed using Pearson coefficient and expressed as its square (R^2). Data are presented as mean \pm SD unless specified otherwise. Bland-Altman analysis and agreement are average difference \pm 2 SD. Comparison of mean differences was performed with an analysis of variance (ANOVA) or Wilcoxon test as appropriate. The F test was used to test the significance of differences in variability. Intraobserver and interobserver variability are presented as mean difference between observations \pm SD. Statistical significance was defined as $p < 0.05$.

RESULTS

Determination of AAR and infarct size. Figure 1 illustrates the image and tissue analysis methodology. AAR was quantified on T1 and T2 maps. Microspheres provided the independent measure of AAR. Infarct size was by TTC. Figure 2 illustrates the regions of interest used to quantify LV mass and AAR on a whole heart by T1 and T2 maps.

Assessment of the infarct model. The blood flow in the core of the occluded area was assessed by microspheres in order to ensure the validity of the infarct model. Blood flow in this area was $6.5 \pm 5.3\%$ of the blood flow in normally perfused remote myocardium. AAR by microspheres was larger than

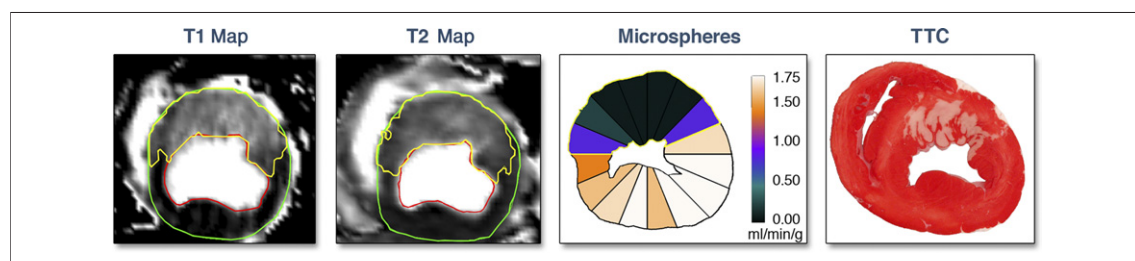


Figure 1. Myocardial Area at Risk by T1 Mapping, T2 Mapping, and Microspheres Compared With Infarct Size

Images are shown for 1 representative short-axis slice. Left ventricular endocardial and epicardial borders are delineated in red and green, respectively. In the images of the T1 map and T2 map, the epicardium and endocardium are delineated and the area at risk (AAR) is identified in yellow. Blood flow from microspheres injected during occlusion are displayed on the contours of the ex vivo slice, for 16 radial sectors that are color coded according to the color scale for blood flow quantification in ml/min/g. Sectors with microsphere blood flow 2 SD below remote myocardium are defined as AAR and appear in the blue to black range of the color scale for this experiment. The triphenyltetrazolium chloride (TTC) image shows noninfarcted myocardium stained red and the region of myocardial infarction is white. Note that the area identified as AAR by T1 mapping and T2 mapping corresponds closely with the results of the microsphere blood flow analysis, suggesting that both imaging sequences agree with microsphere results. Also note how the area of infarction is much smaller than the AAR, indicating substantial salvage.

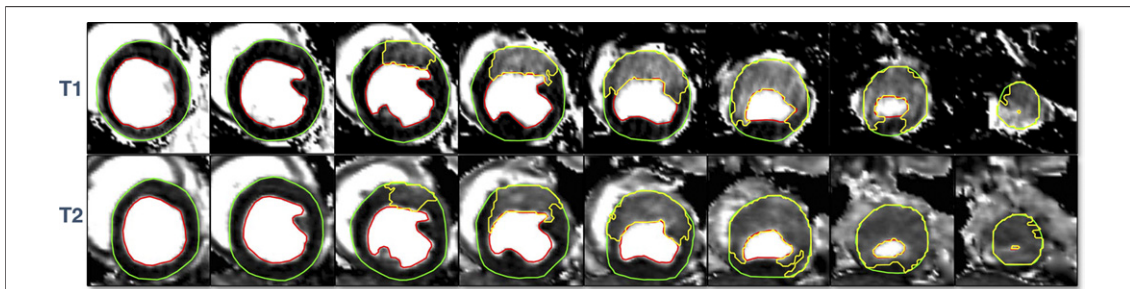


Figure 2. Slice-by-Slice Comparison of T1 and T2 Maps

Short-axis images are shown from the base (left) to the apex (right) for quantification of myocardial area at risk (yellow region of interest). Left ventricular endocardial and epicardial borders are delineated in red and green, respectively. Note the excellent spatial correspondence between the T1 and T2 methods for area at risk.

infarct size by TTC in all cases (AAR $35 \pm 5\%$ of LV myocardium, infarct size $12 \pm 6\%$ of LV myocardium). This yielded a median infarct size of 30% of the AAR (range 12% to 52% AAR), indicating substantial myocardial salvage in this canine model of 2-h coronary occlusion under anesthesia.

Agreement for AAR between T1 and T2 mapping.

Figure 2 illustrates the slice-by-slice agreement for AAR by T1 and T2 mapping for the whole LV. Figure 3 illustrates this quantitatively; AAR by T1 and T2 mapping correlated well ($R^2 = 0.95$, $p < 0.001$). In Bland-Altman analysis (Fig. 3), the measurements of the size of the AAR from T1 and T2 maps agreed well with each other (mean \pm 2 SD: bias $0.4 \pm 16.6\%$ of slice).

Accuracy of LV mass, AAR, and myocardial salvage by T1, T2, and microspheres.

Whole-heart volumetric determinations of LV mass, AAR, and myocardial salvage were determined using each of the 3 methods (Fig. 4). The absolute weight in grams of the total LV myocardium \pm standard error of the mean

(57 ± 2 g, 61 ± 3 g, 62 ± 3 g), AAR (24 ± 2 g, 26 ± 2 g, 23 ± 1 g) was quantified by T1 mapping, T2 mapping, and microspheres, respectively. In terms of the average mass of each zone, there were no statistically significant differences in the size of LV mass by ANOVA ($p = 0.13$). Similarly, none of the measures of AAR ($p = 0.58$) or the amount of myocardial salvage ($p = 0.50$) differed significantly by ANOVA. The patterns of AAR and amount of myocardial salvage were similar for the 3 sets of measurements in absolute grams (Fig. 4).

Intraobserver variability for AAR by T1 and T2 mapping was 0.4 ± 1.3 g ($2.1 \pm 1.8\%$ of LV) and 0.6 ± 2.6 g ($0.6 \pm 3.8\%$ of LV), respectively. Interobserver variability for AAR by T1 and T2 mapping was 1.7 ± 3.9 g ($1.4 \pm 4.6\%$ of LV) and 1.4 ± 4.4 g ($0.3 \pm 5.4\%$ of LV), respectively.

Volumetric T1 measurements of LV mass, AAR, and myocardial salvage correlated to microsphere measures (Fig. 5) ($R^2 = 0.94$). The T1 measure-

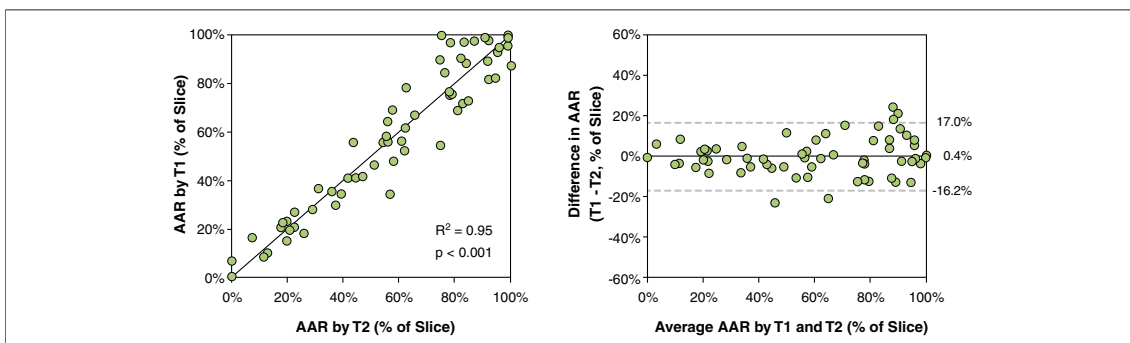


Figure 3. Slice-by-Slice Comparison of Myocardial Area at Risk by T1 Mapping and T2 Mapping

The figure shows a scatterplot (left) and Bland-Altman analysis (right) of myocardial area at risk (AAR) by T1 mapping versus T2 mapping. Data represent 78 slices from 9 dogs. The solid line denotes the line of identity in the scatterplot and the bias in the Bland-Altman plot. Note the excellent agreement between the methods.

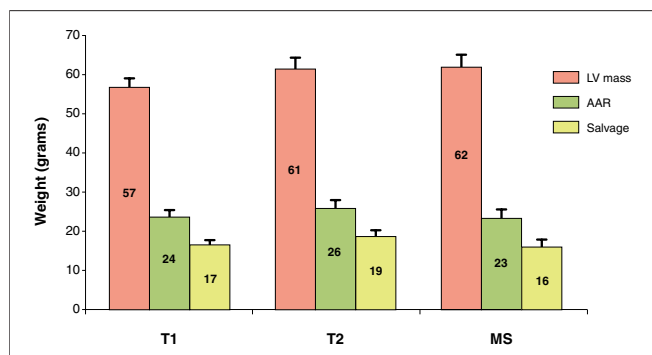


Figure 4. Comparison of Absolute Mass of LV Myocardium, AAR, and Salvaged Myocardium by T1 and T2 Mapping and MS

Error bars denote standard error of the mean. There were no significant differences between the imaging and microsphere (MS) methodologies for the respective measures of left ventricular (LV) mass, area at risk (AAR), or salvage by analysis of variance.

ments showed good agreement in Bland-Altman analysis and tended to underestimate total LV mass marginally (mean \pm 2 SD: bias -1.4 ± 11.2 g of myocardium).

Volumetric T2 measurements of LV mass, AAR, and myocardial salvage also correlated with the microsphere measurements (Fig. 5) ($R^2 = 0.96$). The linear regression was close to the line of

identity. Bland-Altman analysis confirmed the good agreement between T2 and microspheres on a volumetric or mass basis.

T1 and T2 changes directionally consistent with edema. Data on T1 and T2 values in remote and AAR for all animals are presented in Table 1. Both T1 and T2 were greater in AAR compared with remote myocardium.

DISCUSSION

This is the first study to show that in vivo noncontrast T1 mapping by MR imaging can accurately quantify AAR versus an independent microsphere reference standard. In terms of determining area at risk, the T1 mapping method was essentially equivalent to the T2 mapping method. The study confirms our hypothesis that T1 and T2 CMR relaxation properties both change sufficiently to measure AAR. Furthermore, the changes in T1 and T2 are consistent with myocardial edema as a common pathophysiological mechanism leading to the CMR image appearances. This study takes an important step beyond prior work by including whole-heart volumetric measurements of AAR by imaging and microspheres. As is often the case with volumetric

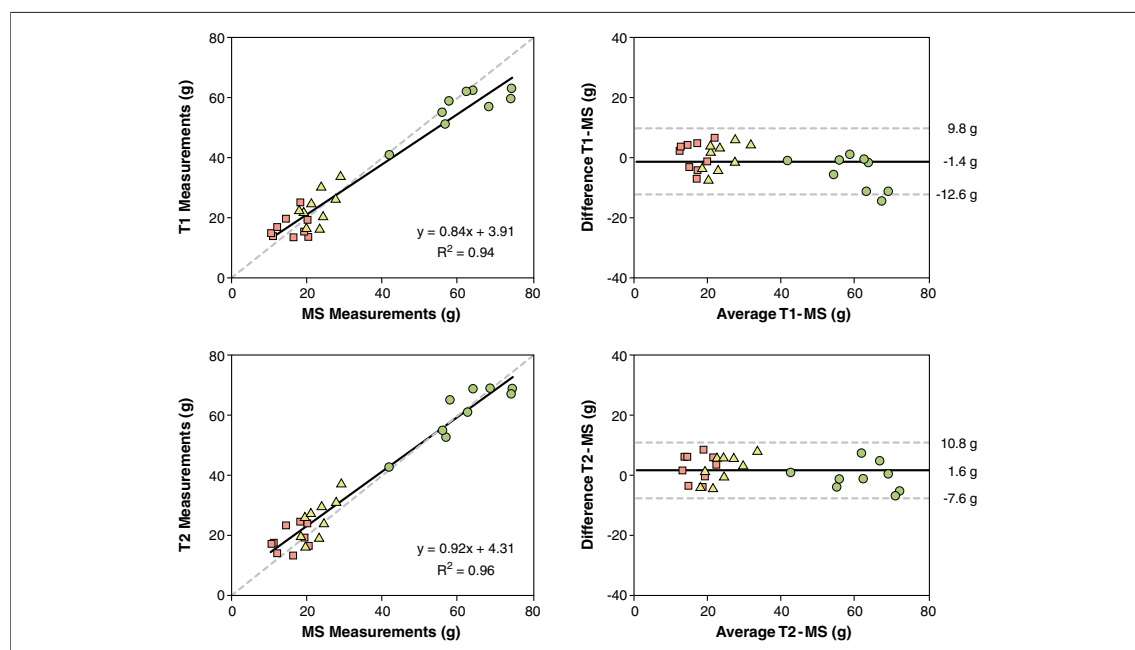


Figure 5. Correlation and Bland-Altman Analysis of Whole-Heart Measures of LV Mass, AAR, and Myocardial Salvage by T1 and T2 Mapping Compared With AAR by MS

Area at risk (AAR) by T1 mapping and T2 mapping are compared with AAR by microspheres (MS) expressed in grams (g). The mean difference between imaging methods and MS was 1.4 g for the T1 measurements and 1.6 g for the T2 measurements. The **dashed lines** denote the line of identity in the scatterplots and the mean \pm 2 SD in the Bland-Altman plots. The following symbols are used for each region of the heart: left ventricular (LV) mass (circles), AAR (triangles), and myocardial salvage (squares).

Table 1. T1 and T2 Values for AAR and Remote Myocardium in All Animals

Animal #	T1 AAR (ms)	T1 Remote (ms)	T2 AAR (ms)	T2 Remote (ms)
1	1,129	914	62	46
2	1,186	961	81	47
3	1,132	899	69	48
4	1,030	857	68	51
5	1,162	924	72	48
6	1,079	891	66	46
7	1,132	910	68	51
8	1,231	903	77	47
9	1,116	971	76	56
Mean	1,133	915	71	49
SD	55	33	6	3

AAR = area at risk.

measurements, the variability of the measurements is smaller compared with prior limited slice-by-slice measurements (6). Finally, the T1 and T2 mapping sequences were developed as works in progress for clinical scanning and thus should be available for quantitative imaging of patients soon.

T2 for quantifying AAR. The utility of T2-weighted CMR in acute cardiac disease has recently been extensively reviewed (20). Several investigators have experimentally determined that T2 increases in proportion to myocardial edema measured as tissue water content (3,21,22). However, the use of T2-weighted CMR for quantifying the AAR was experimentally determined using a T2-weighted double inversion recovery fast spin echo (also called turbo spin echo) sequence compared with microsphere blood flow in the dog for both reperfused (6) and nonreperfused infarcts (5). Subsequently, the T2-weighted imaging methodology has been improved upon with the introduction of T2-prepared SSFP (8), and a T2-prepared hybrid turbo spin echo-SSFP sequence (4). Validation of T2-weighted CMR for quantifying AAR in patients has been performed by comparison with myocardial perfusion single-photon emission computed tomography using either T2-weighted short tau inversion recovery (7), post-gadolinium contrast cine SSFP (9), or T2-prepared SSFP compared with angiographic risk score (23). For purposes of quantitative analysis, image quality in T2-weighted sequences can prove challenging. The current study used a T2-prepared SSFP-based T2 mapping sequence (15) and provides the experimental validation that T2 mapping indeed can accurately quantify the AAR. Furthermore, the T2 values for acute ischemic injury and remote myocardium found in the current

study were similar to those reported in humans and pigs using similar methodology (15,24).

T1 for quantifying AAR. T1-weighted CMR should also be able to detect myocardial edema associated with acute myocardial occlusion and reperfusion. Notably, previous experimental studies have shown that T1 values also increase with increasing myocardial water content (3,11). Furthermore, prolonged T1 values have been experimentally demonstrated in ischemic myocardium in the dog (10), and in patients with acute myocardial infarction (13). However, noncontrast T1-weighted imaging has not previously been used to quantify AAR in vivo, and our current study provides experimental validation that AAR by T1 and T2 mapping agree with microspheres as an independent reference standard.

Agreement between T1 and T2. The current study shows excellent quantitative agreement between T1 and T2 mapping for determining AAR. Previous studies comparing the correlation between myocardial water content and T1 and T2, respectively, have shown results suggesting that T2 has a higher linear correlation (3), indicating that T2 may be the preferred approach for quantifying AAR. However, those results were performed in ex vivo myocardium and using an early-generation 0.35-T CMR scanner, which may have limited signal to noise compared with the current state-of-the-art methods. Importantly, our findings were achieved in vivo using clinical-grade sequences that yield high signal-to-noise image maps.

There are factors that might influence whether one selects T1 or T2 to image AAR. Microvascular obstruction or intramyocardial hemorrhage were absent in our model, but are frequently detectable on T2-weighted images (25). Although this has not yet been studied, these pathophysiological states would be expected to influence pre-contrast T1 to a lesser extent than T2. Quantitative image analysis of T2 maps in such cases would require including the lower T2 regions in the core into total AAR. However, in a setting where it may be of value to assess the myocardial extracellular volume fraction (26), this would require acquiring T1 maps both before and after contrast. It appears that while both mapping techniques provide similar information with regard to AAR, and could be used interchangeably for this purpose, they both provide additional and unique complementary pathophysiologically relevant information.

The infarct model. The current study was performed in a model where infarct size was approximately

30% of AAR and predominantly subendocardial. Acute myocardial infarction changes both T1 and T2 (3,11,21), and the T2 changes represent an area of edema that is larger than the acute infarction and corresponds quantitatively to the AAR (6). Thus, it is important that the experimental model produce infarctions that do not fully encompass the AAR. Our model fulfills this criterion, adding confidence to results indicating that the T1 and T2 mapping methodologies detect changes in the AAR beyond those that are induced by infarction.

Study limitations. Our study only represents changes present at 1 time point about 4 h after reperfusion. Future studies are needed to determine the validity of the quantitative result beyond that time point. Despite this, the time course of myocardial edema between 1 and 7 days post-infarction has been shown to be suitable for detection by CMR (7). The current results were obtained in mechanically ventilated dogs, and translation to human patients may be hampered by challenges related to optimal breath-holding, which may affect the image quality in the T1 or T2 maps. Furthermore, this study did not present segmented data on the mean and SD of

T1 and T2 in healthy noninfarcted dogs, which might be of benefit to determine the robustness of T1 and T2 in truly normal myocardium, and this is a limitation.

CONCLUSIONS

Noncontrast T1 mapping and T2 mapping using clinical-grade sequences show excellent agreement with each other and microsphere blood flow for quantification of AAR following acute myocardial infarction. The relaxation properties T1 and T2 both change in a way that is consistent with the myocardial edema that occurs following myocardial ischemia/reperfusion.

Acknowledgments

The authors thank Joni Taylor and Katherine Lucas for expert animal care.

Reprint requests and correspondence: Dr. Andrew E. Arai, Cardiovascular and Pulmonary Branch, National Heart, Lung, and Blood Institute, National Institutes of Health, 10 Center Drive, Building 10, Room B1D416, Bethesda, Maryland 20892-1061. *E-mail:* arai@nih.gov.

REFERENCES

1. Lowe JE, Reimer KA, Jennings RB. Experimental infarct size as a function of the amount of myocardium at risk. *Am J Pathol* 1978;90:363–79.
2. Basuk WL, Reimer KA, Jennings RB. Effect of repetitive brief episodes of ischemia on cell volume, electrolytes and ultrastructure. *J Am Coll Cardiol* 1986;8:33A–41A.
3. Higgins CB, Herfkens R, Lipton MJ, et al. Nuclear magnetic resonance imaging of acute myocardial infarction in dogs: alterations in magnetic relaxation times. *Am J Cardiol* 1983;52:184–8.
4. Aletras AH, Kellman P, Derbyshire JA, Arai AE. ACUT2E TSE-SSFP: a hybrid method for T2-weighted imaging of edema in the heart. *Magn Reson Med* 2008;59:229–35.
5. Tilak GS, Hsu LY, Hoyt RF Jr., Arai AE, Aletras AH. In vivo T2-weighted magnetic resonance imaging can accurately determine the ischemic area at risk for 2-day-old nonreperfused myocardial infarction. *Invest Radiol* 2008;43:7–15.
6. Aletras AH, Tilak GS, Natanzon A, et al. Retrospective determination of the area at risk for reperfused acute myocardial infarction with T2-weighted cardiac magnetic resonance imaging: histopathological and displacement encoding with stimulated echoes (DENSE) functional validations. *Circulation* 2006;113:1865–70.
7. Carlsson M, Ubachs JF, Hedstrom E, Heiberg E, Jovinge S, Arheden H. Myocardium at risk after acute infarction in humans on cardiac magnetic resonance: quantitative assessment during follow-up and validation with single-photon emission computed tomography. *J Am Coll Cardiol Img* 2009;2:569–76.
8. Kellman P, Aletras AH, Mancini C, McVeigh ER, Arai AE. T2-prepared SSFP improves diagnostic confidence in edema imaging in acute myocardial infarction compared to turbo spin echo. *Magn Reson Med* 2007;57:891–7.
9. Sorensson P, Heiberg E, Saleh N, et al. Assessment of myocardium at risk with contrast enhanced steady-state free precession cine cardiovascular magnetic resonance compared to single-photon emission computed tomography. *J Cardiovasc Magn Reson* 2010;12:25.
10. Williams ES, Kaplan JJ, Thatcher F, Zimmerman G, Knoebel SB. Prolongation of proton spin lattice relaxation times in regionally ischemic tissue from dog hearts. *J Nucl Med* 1980;21:449–53.
11. Brown JJ, Peck WW, Gerber KH, Higgins CB, Strich G, Slutsky RA. Nuclear magnetic resonance analysis of acute and chronic myocardial infarction in dogs: alterations in spin-lattice relaxation times. *Am Heart J* 1984;108:1292–7.
12. Buda AJ, Aisen AM, Juni JE, Gallagher KP, Zotz RJ. Detection and sizing of myocardial ischemia and infarction by nuclear magnetic resonance imaging in the canine heart. *Am Heart J* 1985;110:1284–90.
13. Goldfarb JW, Arnold S, Han J. Recent myocardial infarction: assessment with unenhanced T1-weighted MR imaging. *Radiology* 2007;245:245–50.
14. Messroghli DR, Greiser A, Frohlich M, Dietz R, Schulz-Menger J. Optimization and validation of a fully-integrated pulse sequence for modified look-locker inversion-recovery (MOLLI) T1 mapping of the heart. *J Magn Reson Imaging* 2007;26:1081–6.
15. Giri S, Chung YC, Merchant A, et al. T2 quantification for improved detection of myocardial edema. *J Cardiovasc Magn Reson* 2009;11:56.
16. Messroghli DR, Rudolph A, Abdel-Aty H, et al. An open-source software tool for the generation of relaxation time maps in magnetic resonance imaging. *BMC Med Imaging* 2010;10:16.

17. Heiberg E, Sjogren J, Ugander M, Carlsson M, Engblom H, Arheden H. Design and validation of Segment—freely available software for cardiovascular image analysis. *BMC Med Imaging* 2010;10:1.
18. Heiberg E, Engblom H, Engvall J, Hedstrom E, Ugander M, Arheden H. Semi-automatic quantification of myocardial infarction from delayed contrast enhanced magnetic resonance imaging. *Scand Cardiovasc J* 2005;39:267–75.
19. Hsu LY, Natanzon A, Kellman P, Hirsch GA, Aletras AH, Arai AE. Quantitative myocardial infarction on delayed enhancement MRI. Part I: animal validation of an automated feature analysis and combined thresholding infarct sizing algorithm. *J Magn Reson Imaging* 2006;23:298–308.
20. Eitel I, Friedrich MG. T2-weighted cardiovascular magnetic resonance in acute cardiac disease. *J Cardiovasc Magn Reson* 2011;13:13.
21. Boxt LM, Hsu D, Katz J, et al. Estimation of myocardial water content using transverse relaxation time from dual spin-echo magnetic resonance imaging. *Magn Reson Imaging* 1993;11:375–83.
22. Garcia-Dorado D, Oliveras J, Gili J, et al. Analysis of myocardial oedema by magnetic resonance imaging early after coronary artery occlusion with or without reperfusion. *Cardiovasc Res* 1993;27:1462–9.
23. Berry C, Kellman P, Mancini C, et al. Magnetic resonance imaging delineates the ischemic area at risk and myocardial salvage in patients with acute myocardial infarction. *Circ Cardiovasc Imaging*;3:527–35.
24. Verhaert D, Thavendiranathan P, Giri S, et al. Direct T2 quantification of myocardial edema in acute ischemic injury. *J Am Coll Cardiol Img* 2011;4:269–78.
25. Payne AR, Berry C, Kellman P, et al. Bright-blood T(2)-weighted MRI has high diagnostic accuracy for myocardial hemorrhage in myocardial infarction: a preclinical validation study in swine. *Circ Cardiovasc Imaging* 2011;4:738–45.
26. Ugander M, Oki AJ, Hsu LY, et al. Extracellular volume imaging by magnetic resonance imaging provides insights into overt and sub-clinical myocardial pathology. *Eur Heart J* 2012;33:1268–78.

Key Words: cardiac magnetic resonance ■ ischemia ■ microspheres ■ myocardial infarction ■ myocardium at risk.